

LETTER TO THE EDITOR

A trio of month-long flares in the nova-like variable V704 And

G. Zsidi^{1,2,3} , C. J. Nixon¹, T. Naylor⁴, J. E. Pringle⁵, and K. L. Page⁶ 

¹ School of Physics and Astronomy, Sir William Henry Bragg Building, Woodhouse Ln., University of Leeds, Leeds LS2 9JT, UK
e-mail: g.zsidi@leeds.ac.uk

² Konkoly Observatory, Research Centre for Astronomy and Earth Sciences, Eötvös Loránd Research Network (ELKH),
Konkoly-Thege Miklós út 15-17, 1121 Budapest, Hungary

³ CSFK, MTA Centre of Excellence, Budapest Konkoly Thege Miklós út 15-17, 1121 Budapest, Hungary

⁴ School of Physics and Astronomy, University of Exeter, Stocker Road, Exeter EX4 4QL, UK

⁵ Institute of Astronomy, University of Cambridge, Madingley Road, Cambridge CB3 0HA, UK

⁶ School of Physics and Astronomy, University of Leicester, Leicester LE1 7RH, UK

Received 12 May 2023 / Accepted 11 August 2023

ABSTRACT

We present the discovery of an unusual set of flares in the nova-like variable V704 And. Using data from AAVSO, ASAS-SN, and ZTF for the nova-like variable V704 And, we discovered a trio of brightening events that occurred during the high state. These events elevate the optical brightness of the source from ~ 13.5 to ~ 12.5 mag. The events last for roughly a month, and exhibit the unusual shape of a slow rise and faster decay. Immediately after the third event, we obtained data from regular monitoring with *Swift*, although by this time the flares had ceased and the source returned to its pre-flare level of activity in the high state. The *Swift* observations confirm that during the high state, the source is detectable in the X-rays, and provide simultaneous UV and optical fluxes. As the source is already in the high state prior to the flares, and therefore the disc is expected to already be in the high-viscosity state, we conclude that the driver of the variations must be changes in the mass transfer rate from the companion star and we discuss mechanisms that could lead to such short-timescale mass-transfer variations.

Key words. stars: individual: V704 And – accretion, accretion disks – novae, cataclysmic variables

1. Introduction

Cataclysmic variables (CVs) are close interacting binary systems in which a white dwarf is accreting material from a companion via Roche-lobe overflow. In the case of weakly or non-magnetic CVs, the material transferred from the secondary component forms an accretion disc around the primary. These systems may be classified based on their photometric and spectroscopic characteristics (Warner 1995). For example, dwarf novae (DNe) show recurring accretion-related outbursts – and sometimes superoutbursts – lasting from a few days to ~ 20 days. The nova-like variables (NLs), defined as those that do not display nova or DN outbursts, remain in a state of high accretion, and therefore in a bright photometric state, for a prolonged time.

The VY Sculptoris stars (also called ‘antidwarf novae’) are an interesting subclass of NLs whose bright photometric states are occasionally interrupted by rapid drops in brightness (low states). The low states are believed to be caused by decreased mass transfer from the companion, which can eventually lead to the disappearance of the disc (Hameury & Lasota 2002). However, it is argued that sometimes the accretion disc does not disappear completely during these periods (Schmidtobreick et al. 2018). The exact process causing the reduced mass transfer is still unknown, but one mechanism that was suggested by previous works is starspots on the secondary that block the L1 point and therefore suppress the mass transfer (Livio & Pringle 1994).

V704 Andromedae – hereafter referred to as V704 And – is a poorly studied NL; its variable nature was discovered only roughly two decades ago by Dahlmarm (1999), who

reported brightness changes in the *V* band between 14.8 and 12.6 mag. The source was further studied in the early 2000s by Papadaki et al. (2006) within a photometric survey of little-studied CVs, mainly focusing on nova-like variables. Based on optical photometric measurements between 2002 and 2005, these authors found that V704 And showed fading episodes in 2003 and 2005. Long-term historical light curves confirm the occasional fading of the system, which suggests that V704 And belongs to the VY Scl subclass of the nova-like variables, and the optical study by Weil et al. (2018) supports this argument. Bruch (2022) further investigated the system and measured an orbital period of $P_{\text{orb}} = 0.15424(3)$ days (3.7 h). This is within the typical range of orbital periods for VY Scl nova-like variables. Furthermore, Bruch (2022) estimated the spectral type of the secondary to be M3–M4 using optical spectra obtained during a low state. These authors revealed a strong negative superhump in the V704 And system by analysing the Transiting Exoplanet Survey Satellite (TESS) light curves with a period of $P_{\text{nSH}} = 0.14772(3)$ days. The system was also included in the *Gaia* survey, which placed it at a distance of $410.4^{+6.3}_{-5.3}$ pc (Bailer-Jones et al. 2021).

2. Observations

In order to analyse the long-term behaviour of V704 And, we inspected photometric data from public surveys. We studied the data obtained by ZTF (Bellm et al. 2019), which is designed to observe the northern sky with an approximately two-day

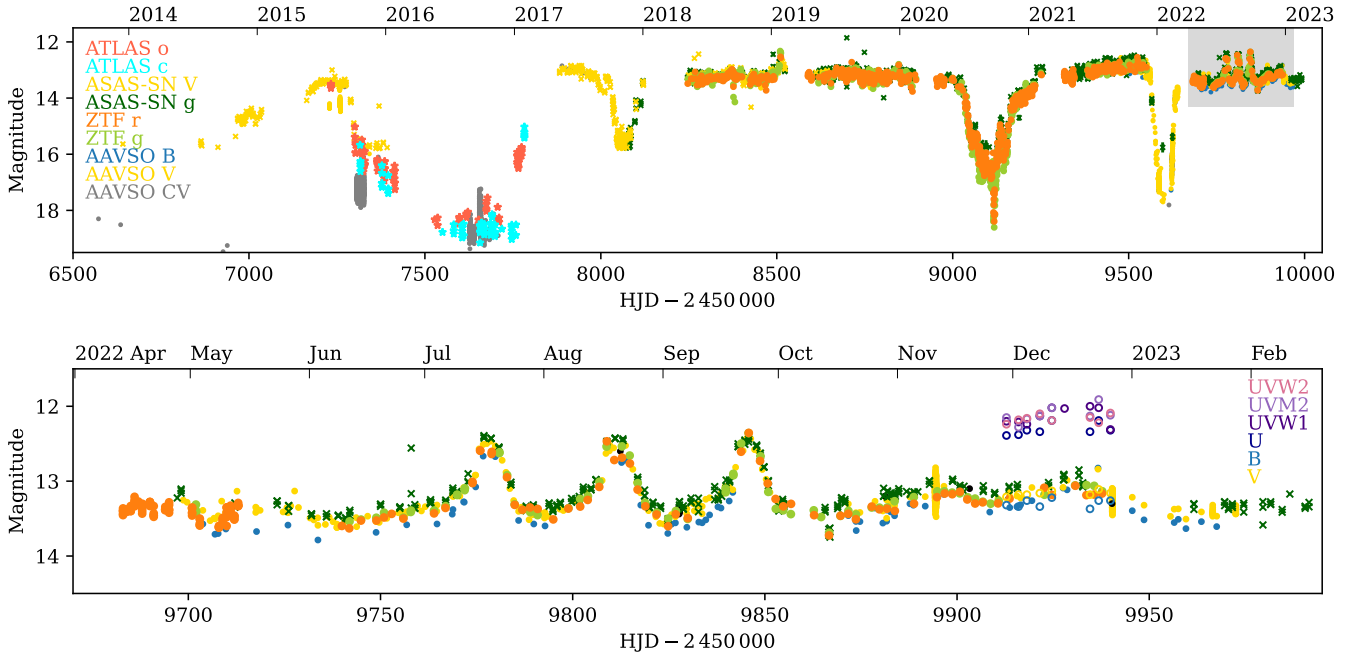


Fig. 1. Light curves of V704 And. *Top panel:* optical light curves of V704 And. The yellow and dark green x -symbols show the ASAS-SN V and g band measurements, the orange and the light green filled circles indicate the ZTF r and g band observations; and yellow, blue, and grey circles mark the AAVSO B , V band, and unfiltered CCD (CV) measurements, respectively. The cyan and dark orange star symbols are measurements from the ATLAS survey with the c and o filters, respectively. The grey shaded area indicates the period shown in the bottom panel. We note that the ATLAS measurements from 2016 suggest that the system was as faint as ~ 18 mag during this period; however, the ASAS-SN data indicate a brightness of around 16 mag. As the sensitivity of ATLAS observations is higher, and the ASAS-SN measurements from this period include several upper-limit measurements, we exclude those ASAS-SN data that are fainter than 16 mag from the figure. *Bottom panel:* optical and UV measurements obtained since 2022 April (grey shaded area in the top panel). The empty circles show the *Swift* optical and UV data. Yellow, blue, and black filled circles are the AAVSO V , B , and visual band observations, respectively.

cadence. We downloaded the measurements for V704 And from their archive¹, which provided photometric measurements between 2018 March and 2023 January in the Palomar/ZTF g and r bands for the latest data release (DR16). In order to remove poor-quality observations, we applied the ‘catflags=0’ filter of the catalogue. Johnson V and Sloan g band photometric observations are also available from the ASAS-SN survey. The ASAS-SN team performs aperture photometry using a two-pixel aperture radius, and the reduced data are available from their online catalogue². V band measurements were obtained between 2013 December and 2018 August, whereas the g band observations are available since 2017 December (Kochanek et al. 2017; Shappee et al. 2014). Despite both surveys providing g band data, we analysed them separately as the sensitivity differs between the two surveys: the ASAS-SN is sensitive up to ~ 17 mag, whereas the ZTF is accurate up to about 20.8 mag. We also complemented our dataset with observations from the ATLAS survey (Heinze et al. 2018), which provided measurements in ‘cyan’ and ‘orange’ filters³ between 2015 and 2017, which have a sensitivity of up to ~ 19 mag. Furthermore, we examined the AAVSO optical light curves of V704 And, which date back to 1966 and allow us to study the historic behaviour of the system. However, we must note that the early AAVSO observations for V704 And are incomplete, and the observers either do not provide information on the filter used, or applied a ‘visual’

band. The more recent measurements often provide Johnson B or V band observations in addition to the visual ones⁴.

We also monitored V704 And with the Ultraviolet/Optical Telescope (UVOT) instrument of the *Swift* satellite between 2022 November 29 and December 26 with a three-day cadence (ToO ID 18163, PI: G. Zsidi). We used the ‘0 \times 30ed’ mode of UVOT, which provided photometric measurements in the V , B , and U optical and the $UVW1$, $UVM2$, and $UVW2$ UV filters⁵. However, due to a scheduling conflict, one observation was not executed, and the one on 2022 December 14 was carried out only in the $UVW1$ filter. We reduced the UVOT data using the version 6.31.1 of the HEASOFT software. All UV and optical light curves are displayed in Fig. 1.

3. Results

The brightness of V704 And varies around 13 mag in the high state but this is occasionally interrupted by low-state periods during which the brightness of the system decreases by 3–5 mag. According to the most recent optical ASAS-SN and the ZTF light curves (Fig. 1, top panel), V704 And underwent three low-state periods over the last six years (i.e., since 2017), each of which lasted about six months. Before 2017, the system exhibited an inverse behaviour to some extent, as it spent a longer period of time in the low-brightness state. This behaviour is characteristic of the system since the mid-2000s, as revealed by the AAVSO light curves (Fig. A.1). Despite the fact that the AAVSO

¹ <https://irsa.ipac.caltech.edu/Missions/ztf.html>

² <https://asas-sn.osu.edu/>

³ The “cyan” (c) filter covers the 420–650 nm wavelength range, and the “orange” (o) filter covers the 560–820 nm band.

⁴ <https://www.aavso.org/filters>

⁵ Central wavelengths of the UVOT filters (\AA): V – 5468, B – 4392, U – 3465, $UVW1$ – 2600, $UVM2$ – 2246, $UVW2$ – 1928.

observations date back to 1966, the early measurements were rather incomplete, and therefore we cannot make far-reaching conclusions about the historical behaviour of the system. The available data suggest that V704 And spent significant time in the high state between 1966 and 1995, but intervening drops into the low state during this time cannot be ruled out.

3.1. The trio of flares in the latest high state

The most recent low state of V704 And finished around 2022 March or April. The source initially returned to a regular high state for a few months, albeit at a slightly lower flux level than before the latest minimum ($g \approx 13.5$ mag rather than $g \approx 12.8$ mag prior). However, the system then began to show peculiar outburst-like events – which we refer to as flares in order to distinguish them from ordinary CV outbursts – with amplitudes of ~ 1 mag and lasting for about a month each. The bottom panel of Fig. 1 shows an enlarged excerpt of the light curve highlighting these events. The outbursts seem to have an asymmetric evolution: it takes 18–20 days to reach the maximum, and 10–12 days to return to the initial brightness level⁶.

The light curves of the flares obtained with different filters are remarkably similar; we did not detect any noticeable time delay in reaching the maximum brightness at different wavelengths. This might be caused by two factors. One is that, due to the cadence of the light curves, the peaks of the flares are not well defined in all filters. The other cause could be that the available optical filters indeed probe the same region of the system; therefore, no time delay is expected in these observations.

It is instructive to compare the outbursts of V704 And with the DNe outbursts. The two types of outbursts might look similar in amplitude and in length, but the DN outbursts normally exhibit an asymmetry with an opposite trend; that is, they show faster rise than decay (Cannizzo et al. 1986). Furthermore, the increase in the far-UV flux can be delayed compared to the optical. However, this second aspect cannot be probed for V704 And, as we only have optical light curves during the flares.

3.2. Colour changes

The multi-filter photometric observations allow us to examine the colour variations of V704 And. The ZTF survey provides sufficiently long coverage to study the changes in the system on a yearly timescale. We constructed the colour–magnitude diagram using the simultaneous g and r band measurements (Fig. 2). Our results show that when the object is in the low and fainter state, the data points cover a wider range in the colour space. However, as the system brightens, the overall colour is more concentrated on the blue side.

It is interesting to separate those observations when the system undergoes the three flares in order to investigate their nature. For this reason, we highlight the data points that cover the period between HJD–2450000 = 9740 and 9890 with orange symbols. Furthermore, we indicate the earlier measurements with darker shades and the later ones with lighter shades in order to investigate the temporal evolution. We find that no significant colour change is observed when V704 And brightens by ~ 1 mag. However, we must note that the simultaneous g and r band data do not cover the flares entirely.

⁶ We also note that around HJD–2450000 = 8500, V704 And exhibited a small-amplitude brightening event. However, due to the sparseness of the data during that period, it is not possible to tell with certainty whether this event was similar to the trio of flares in 2022.

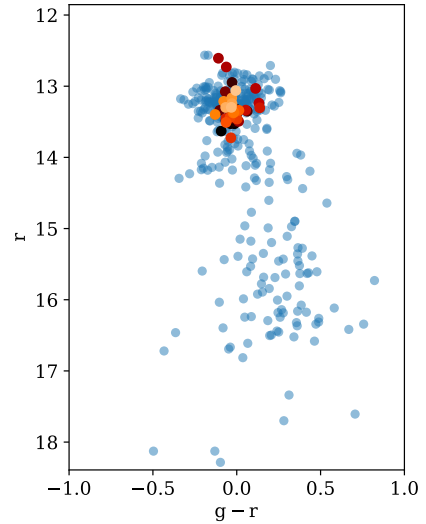


Fig. 2. Optical colour–magnitude diagram based on the ZTF measurements. The blue filled circles show the entire dataset, whereas the orange ones cover only the period between JD–2450000 = 9740 and 9890, i.e., when the three flares occurred. The measured errors are smaller than or equal to the symbol size.

The *Swift* measurements provide information on the colour of the high state after the trio of flares. During this time, the brightness of the system does not change substantially. Figure E.1 shows that no significant colour change is detected in the optical filters. The most apparent evolution is observed at the shortest wavelengths (*UVM2* and *UVW2* filters), in which the system becomes redder as it brightens.

4. Discussion

V704 And is a nova-like variable star that typically displays a steady high-state brightness corresponding to $g \approx 13$ – 13.5 mag, with aperiodic low states lasting several months. In the high-state, the accretion disc shows no evidence for DNe-type outbursts, and therefore the whole disc is expected to be fully ionised with well-established hydro-magnetic viscosity. In similar systems, primarily the DNe in outburst, the disc viscosity parameter α (Shakura & Sunyaev 1973) is found to be high with $\alpha \approx 0.2$ – 0.4 (Martin et al. 2019). As the disc is already in the high state for the months preceding the trio of flares, it is unlikely that these flares are caused by variations in α . Instead, they are likely to be caused by variations in the accretion rate through the disc, which is controlled by the mass supply rate from the companion star. To determine whether the duration of the flares is consistent with varying mass supply to the outer disc regions, we computed the viscous timescale in V704 And, which we discuss below. We then discuss possible mechanisms that could induce a change to the mass-transfer rate in this system.

4.1. Viscous timescale in V704 And

The timescale on which the central accretion rate responds to changes in the mass-transfer rate from the companion star is the viscous timescale given by $t_v = R^2/\nu$. Here, ν is the Shakura & Sunyaev (1973) kinematic viscosity and R is the radius in the disc at which the mass transferred from the companion star is added. For our estimate, we take this to be the outer disc edge where viscous spreading of the disc is impeded by tides from the companion star. To evaluate R and ν , we require

estimates for the system parameters; for example, M_1 , M_2 , P_{orb} , and \dot{M} .

The estimates of the system parameters can be uncertain, and therefore we only summarise here the main steps of the calculation. Our detailed calculation and the estimates of the system parameters can be found in Appendix C. Using $P_{\text{orb}} = 0.15424(3)$ days, $q = 0.34$, $M_2 = 0.3 M_{\odot}$, and $M_1 = 0.9 M_{\odot}$, we find a binary separation of $a = 8.9 \times 10^{10}$ cm, and therefore the outer disc radius is $R \approx 2.3 \times 10^{10}$ cm. We also assume a typical white dwarf radius of $R = 0.01 R_{\odot}$, and take $\alpha = 0.3$. Using Eq. (5.50) in Frank et al. (2002), we then estimate the viscous timescale through the disc to be 9.6 days for an accretion rate of $5 \times 10^{-9} M_{\odot} \text{ yr}^{-1}$, and 7.7 days for an accretion rate of $10^{-8} M_{\odot} \text{ yr}^{-1}$. We therefore conclude that the viscous timescale is approximately a week, and maybe up to 10 days. This timescale is consistent with the breadth of the flares, and also consistent with the viscous timescale inferred from measurements of the decay of DNe light curves (e.g., Cannizzo 1994).

4.2. Origin of the flares

The origin of the flares is puzzling. At the optical wavelength range, the accretion disc is the most dominant component of a NL system in a high state (Pringle & Wade 1985); however, disc instability typical of DNe is an unlikely cause of the observed flares of V704 And, as their characteristics differ from DN outbursts. We propose that variable mass transfer from the secondary is responsible for inducing the flares. Nonetheless, VY Scl type variables are expected to have the highest mass-transfer rate during the high state (Warner 1987). For this reason, there has to be an additional mechanism that induces the increase in the mass-transfer rate. Here, we discuss a few mechanisms to achieve this.

Variability in the mass-transfer rate can be achieved by variations of the radius of the secondary (Warner 1988; King et al. 1995). King et al. (1995) propose that variable irradiation by the accreting component may induce changes in the radius of the Roche lobe-filling star, which causes a limit-cycle variation. However, the timescale of this is significantly longer (10^5 – 10^6 yr) than the variations we see here. Another mechanism that could contribute to the variation of the radius of the secondary component is solar-type magnetic cycles. Warner (1988) report such quasi-periodic variations in CVs but these also appear on timescales of several years.

Magnetic activity, at the same time, can have short-term effects as well (Baliunas & Vaughan 1985). The light curves of main sequence stars often reveal the presence of star spots and flares, and as the secondaries of CVs are main sequence stars, stellar activity is expected in these systems as well. Indeed, Webb et al. (2002), for example, found spectroscopic evidence for starspots on the secondary star of SS Cyg, and Dunford et al. (2012) found a high-latitude starspot on RU Peg with Roche tomography. Flares or coronal mass ejections of the secondaries of a CV may induce additional, large amounts of matter, but we cannot directly test this theory for V704 And, as the optical light curves of CVs are dominated by the emission from the disc, which veils the variability of any stellar activity.

4.3. Comparison with other VY Scl-type systems

We compiled a list of VY Scl-type NLs and examined their short- and long-term light curves based on AAVSO, ZTF, and ASAS-SN observations with the aim of looking for any similar behaviour to that observed in V704 And. The majority of these objects are taken from Table 4.1 of Warner (1995), which we

complemented with a few additional systems that were identified as VY Scl-type NLs since that table was compiled; see our complete list of the inspected objects in Table D.1. We find that most of these systems behave as typical VY Scl-type objects with high states occasionally interrupted by low states. We identified only a few systems that show any kind of outburst-like events (see Fig. D.1). For example, the light curves of HV And, BZ Cam, LQ Peg, and HS 0506+7725 each reveal a small-amplitude brightening, but these events show more complex structure than those of V704 And. In contrast, V1082 Sgr and VZ Scl show more stochastic brightness variations.

When individual outbursts are examined, some VY Scl-type systems show superficial similarities to the flares of V704 And. Certain brightening events in the light curves of FY Per, CM Del, or LN UMa seem to have similar duration and/or amplitude to the flares seen in the light curves of V704 And. However, there are significant differences between V704 And and these other NLs. Firstly, the shape, amplitude, and duration of the brightening events of the latter vary from outburst to outburst, whereas the three flares of V704 And are remarkably similar. This is also supported by the high-cadence TESS light curve of FY Per (Fig. D.4), which, as opposed to the flares in V704 And, shows a faster rise than its decay. Secondly, the long-term light curves reveal that the outbursts can be continuously present in the light curves of FY Per and CM Del over timescales of decades (see Fig. D.2), which is best revealed by the higher-cadence ASAS-SN and ZTF data; in contrast, V704 And displayed three identical flares over a period of three months.

Among the sources that show features that are superficially similar to the V704 And flares, LN UMa appears to be the closest match. LN UMa shows alternating low states and high states, typical of a VY Scl-type object (Hillwig et al. 1998). However, over the last decade, the light curve of LN UMa appears significantly more variable than the regular high states of V704 And. In particular, the high states of LN UMa are often interrupted by a series of outburst-like events, which can remain present for an extended period of time. This behaviour is not characteristic of VY Scl-type objects, and to our knowledge has not been reported for this source in the literature before. It is tempting to assign to the outbursts seen in the LN UMa light curve the same physical mechanism as for the flares seen in V704 And. However, we note that the accretion rate of LN UMa is likely to be very close to the critical accretion rate for disc instability; using the 974_{-21}^{+22} pc distance measured by Gaia (Bailer-Jones et al. 2021) and the correlation between the absolute magnitude of the disc and the accretion rate (see Eq. (7) in Puebla et al. 2007) yields an estimate for the accretion rate that (depending on the system inclination) can be above or below the critical accretion rate. As such, it is not currently possible to decide with any certainty whether LN UMa is above, on, or below the critical accretion rate, and therefore we cannot be confident which physical effect is responsible for the variability in the LN UMa light curve.

Some of the above-mentioned NLs (e.g., FY Per, V794 Aql) are known to exhibit quasi-periodic stunted outbursts⁷, which could be caused by a variety of mechanisms, which include mass transfer modulations, DN-type outbursts, DN-type outbursts in a truncated disc, or Z Cam-like outbursts (Honeycutt et al. 1998). Honeycutt (2001) argues that among these, the accretion disc instability is the favoured driving mechanism. More recent works show strong indications that some of the stunted outbursts are caused by mass-transfer variations (see e.g., Robertson et al. 2018).

⁷ The cadence of the light curve for V794 Aql is insufficient to accurately characterise the shape of the outbursts (see Fig. D.1).

However, these latter authors remain uncertain of the nature of the stunted outbursts due to discrepancies between their findings, as some of the results could be explained by both mass transfer variations and accretion disc instability related to the Z Cam phenomenon. The contradiction regarding the origin of the stunted outburst is also discussed in a review by Hameury (2020).

As some of the outbursts in the repeating systems (particularly FY Per, LN UMa, and CM Del) show some similarity to the three isolated flares in V704 And, it is possible that the same mechanism is driving both phenomena, including the stunted outbursts. If these phenomena are all caused by the same mechanism, then, for the reasons laid out in Sect. 4.2, this leads to the conclusion that the stunted outbursts and the variability in, for example, CM Del are driven by mass-transfer variations rather than disc instability. However, we emphasise that there are significant differences between the three flares seen in V704 And and the variability we find in other systems; notably the typical shape and number of the events. For this reason, we conclude that the flares reported here in V704 And are more likely to be physically distinct and therefore could in principle be driven by a different mechanism.

In conclusion, the flare nature observed in V704 And is extraordinary; not only does it differ from the DN outbursts, but no similar behaviour has previously been reported in other VY Scl type NLs. The light curves of V704 And show typical VY Scl type behaviour, with a constant brightness in the high state, occasionally interrupted by short periods of low states. As the system recovered from the latest low state in 2022, it re-established its regular high state. However, instead of remaining at the usual high-state brightness level, it exhibited three flares, and only then did it return to the usual plateau of the high state (see lower panel of Fig. 1). This makes V704 And the first clear example of a system that exhibits flares on the plateau of the high state.

5. Conclusions

Here, we report the discovery of a trio of flares occurring during the high state of the VY Scl-type variable V704 And, behaviour which has never been reported for a nova-like system before. The observed phenomenon also differs from the DN outbursts, and is therefore unlikely to be caused by disc instability. Here, we propose that the flares are caused by increased mass transfer from the secondary and suggest a few possible mechanisms – such as stellar activity of the secondary – that could induce it even when the system is already in the high state. Future observations of V704 And during a prolonged minimum would be desirable, and would allow a better understanding of the nature and activity of the secondary star.

Acknowledgements. We thank the referee for useful comments which helped to improve the manuscript. We thank Phil Evans for providing technical support

with the installation of the *Swift* data analysis software. This work made use of data supplied by the UK *Swift* Science Data Centre at the University of Leicester. GZs and CJN acknowledge support from the Leverhulme Trust (grant number RPG-2021-380). CJN acknowledges support from the Science and Technology Facilities Council (grant number ST/Y000544/1). KLP acknowledges the support from the UK Space Agency. We acknowledge with thanks the variable star observations from the AAVSO International Database contributed by observers worldwide and used in this research.

References

- Bailer-Jones, C. A. L., Rybizki, J., Fouesneau, M., Demleitner, M., & Andrae, R. 2021, *AJ*, 161, 147
- Baliunas, S. L., & Vaughan, A. H. 1985, *ARA&A*, 23, 379
- Bellm, E. C., Kulkarni, S. R., Graham, M. J., et al. 2019, *PASP*, 131, 018002
- Bruch, A. 2022, *MNRAS*, 514, 4718
- Cannizzo, J. K. 1994, *ApJ*, 435, 389
- Cannizzo, J. K., Wheeler, J. C., & Polidan, R. S. 1986, *ApJ*, 301, 634
- Dahlmark, L. 1999, *Inf. Bull. Variable Stars*, 4734, 1
- Downes, R. A., Webbink, R. F., Shara, M. M., et al. 2001, *PASP*, 113, 764
- Dunford, A., Watson, C. A., & Smith, R. C. 2012, *MNRAS*, 422, 3444
- Eggleton, P. P. 1983, *ApJ*, 268, 368
- Evans, P. A., Beardmore, A. P., Page, K. L., et al. 2009, *MNRAS*, 397, 1177
- Frank, J., King, A., & Raine, D. J. 2002, *Accretion Power in Astrophysics*, 3rd edn. (Cambridge: Cambridge University Press)
- Hameury, J. M. 2020, *AdSpR*, 66, 1004
- Hameury, J. M., & Lasota, J. P. 2002, *A&A*, 394, 231
- Heinze, A. N., Tonry, J. L., Denneau, L., et al. 2018, *AJ*, 156, 241
- Henden, A. A., & Honeycutt, R. K. 1995, *PASP*, 107, 324
- Hillwig, T. C., Robertson, J. W., & Honeycutt, R. K. 1998, *AJ*, 115, 2044
- Honeycutt, R. K. 2001, *PASP*, 113, 473
- Honeycutt, R. K., & Kafka, S. 2004, *AJ*, 128, 1279
- Honeycutt, R. K., Robertson, J. W., & Turner, G. W. 1998, *AJ*, 115, 2527
- Honeycutt, R. K., Kafka, S., & Robertson, J. W. 2014, *AJ*, 147, 10
- King, A. R., Frank, J., Kolb, U., & Ritter, H. 1995, *ApJ*, 444, L37
- Kochanek, C. S., Shappee, B. J., Stanek, K. Z., et al. 2017, *PASP*, 129, 104502
- La Dous, C. 1991, *A&A*, 252, 100
- Lasota, J. P., Dubus, G., & Kruk, K. 2008, *A&A*, 486, 523
- Livio, M., & Pringle, J. E. 1994, *ApJ*, 427, 956
- Lyons, K., Stys, D., Slevinsky, R., Sion, E., & Wood, J. H. 2001, *AJ*, 122, 327
- Martin, R. G., Nixon, C. J., Pringle, J. E., & Livio, M. 2019, *New Astron.*, 70, 7
- Papadaki, C., Boffin, H. M. J., Sterken, C., et al. 2006, *A&A*, 456, 599
- Pecaut, M. J., & Mamajek, E. E. 2013, *ApJS*, 208, 9
- Pringle, J. E., & Wade, R. A. 1985, *Interacting Binary Stars* (Cambridge: Cambridge University Press)
- Puebla, R. E., Diaz, M. P., & Hubeny, I. 2007, *AJ*, 134, 1923
- Ricker, G. R., Winn, J. N., Vanderspek, R., et al. 2015, *J. Astron. Telesc. Instrum. Syst.*, 1, 014003
- Ritter, H., & Kolb, U. 2003, *A&A*, 404, 301
- Robertson, J. W., Honeycutt, R. K., Henden, A. A., & Campbell, R. T. 2018, *AJ*, 155, 61
- Schmidtobreick, L., Mason, E., Howell, S. B., et al. 2018, *A&A*, 617, A16
- Schwope, A. D., & Reinsch, K. 1992, *Inf. Bull. Variable Stars*, 3725, 1
- Shakura, N. I., & Sunyaev, R. A. 1973, *A&A*, 24, 337
- Shappee, B. J., Prieto, J. L., Grupe, D., et al. 2014, *ApJ*, 788, 88
- Warner, B. 1987, *MNRAS*, 227, 23
- Warner, B. 1988, *Nature*, 336, 129
- Warner, B. 1995, *Cataclysmic Variable Stars* (Cambridge: Cambridge University Press), 28
- Webb, N. A., Naylor, T., & Jeffries, R. D. 2002, *ApJ*, 568, L45
- Weil, K. E., Thorstensen, J. R., & Haberl, F. 2018, *AJ*, 156, 231
- Wood, M. A., Thomas, D. M., & Simpson, J. C. 2009, *MNRAS*, 398, 2110

Appendix A: AAVSO light curve of V704 And

AAVSO has been carrying out observations of V704 And since 1966. We show the entire available AAVSO light curve for V704 And in Fig. A.1.

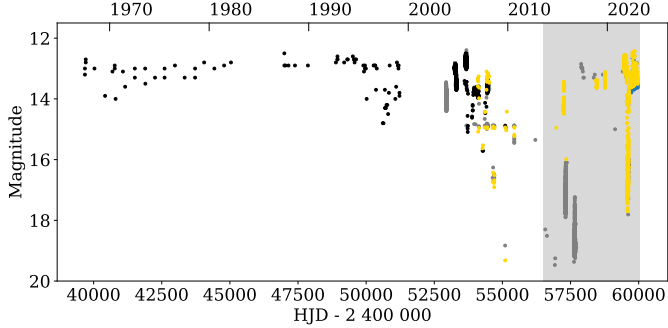


Fig. A.1. AAVSO optical light curves of V704 And. The yellow, blue, black, and grey circles show the B, V, visual, and unfiltered CCD measurements, respectively. We indicate the period with the grey shaded area, which is shown in the top panel of Fig. 1.

Appendix B: Swift X-ray observations

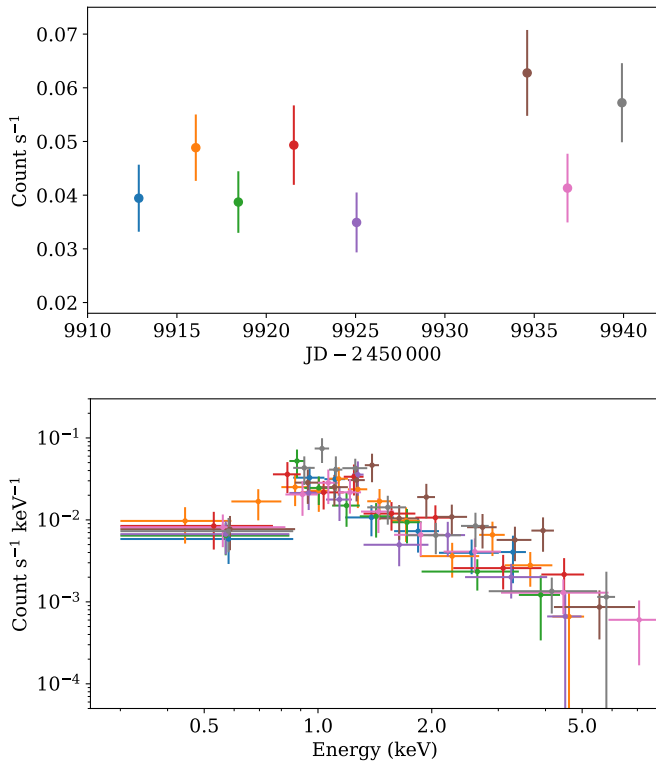


Fig. B.1. X-ray observations of V704 And. *Top*: XRT light curve. *Bottom*: XRT spectra. The different colours correspond to the spectra taken at the different epochs, as in the top panel.

The Swift satellite also provided X-ray measurements obtained by the X-Ray Telescope (XRT; operating in the 0.3 – 10 keV range) contemporaneously with the UVOT observations. The X-ray data were obtained in photon counting mode for about 1.5 ks each. The spectra were created using the XRT online product generator (Evans et al. 2009), which provided the X-ray count

rate and spectrum for each epoch. We show the XRT light curve in Fig. B.1, which does not reveal high variability during the time of the observations. The brightness of the source fluctuates around 0.05 counts s^{-1} . We show the X-ray spectra in the bottom panel of Fig. B.1. The different colours correspond to the spectra taken at the different epochs.

Appendix C: Confirmation of the viscous timescale in V704 And

In order to confirm the viscous timescale of V704 And, we require estimates for the system parameters; for example, M_1 , M_2 , P_{orb} , and \dot{M} . The orbital period was measured by Bruch (2022) as $P_{\text{orb}} = 0.15424(3)$ days. To estimate the primary and secondary masses, we use the superhump period to determine the mass ratio and the spectral type of the secondary to determine M_2 . Wood et al. (2009) present a relationship between the mass ratio $q = M_2/M_1$, the orbital period, and the negative superhump period deficit $\varepsilon_- = (P_{\text{nSH}} - P_{\text{orb}})/P_{\text{orb}}$. Using the P_{orb} and P_{nSH} values determined by Bruch (2022), the mass ratio for the system is $q = 0.34$. Weil et al. (2018) estimate the spectral type of the secondary to be M3–M4, and based on this we can estimate the mass of the secondary to be around $0.3M_{\odot}$ ⁸ (Pecaut & Mamajek 2013).⁹ Combined with the mass ratio of $q = 0.34$, this means that the mass of the white dwarf is $M_1 = 0.9M_{\odot}$.

To estimate the accretion rate through the disc, we use the weak correlation between P_{orb} and \dot{M} (Puebla et al. 2007, see also Warner 1987), which suggests $\dot{M} \approx 5 \times 10^{-9} M_{\odot}/\text{yr}$. As this is a weak correlation, we expect that values of up to $\dot{M} \approx 10^{-8} M_{\odot}/\text{yr}$ are plausible, and so we provide a range of timescales based on a range of accretion rates below. We note that these accretion rates result in a surface temperature of $\approx (2 - 3) \times 10^4$ K in the outer disc regions, which is sufficient to ensure that the source remains in the high state without exhibiting DN like outbursts. Furthermore, the absolute magnitude of V704 And is comparable to other members of the VY Scl type variables, which also supports the argument that the high state of V704 And is similar to that of other prolonged high states of this class.

Frank et al. (2002) provide the outer radius of the disc due to tides as $R \approx 0.9R_{\text{RL}}$ (their equation 5.122), where R_{RL} is the Roche lobe radius given by (Eggleton 1983)

$$\frac{R_{\text{RL}}}{a} = \frac{0.49q^{2/3}}{0.6q^{2/3} + \ln(1 + q^{1/3})}, \quad (\text{C.1})$$

where a is the binary separation. From the period and masses given above, we find a binary separation of $a = 8.9 \times 10^{10}$ cm, and therefore the outer disc radius is $R \approx 2.3 \times 10^{10}$ cm.

Finally, we assume a typical white dwarf radius of $R = 0.01R_{\odot}$, and take $\alpha = 0.3$. Then using equation 5.50 in Frank et al. (2002), we estimate the viscous timescale through the disc to be 9.6 days for an accretion rate of $5 \times 10^{-9} M_{\odot}/\text{yr}$, and 7.7 days for an accretion rate of $10^{-8} M_{\odot}/\text{yr}$. We therefore conclude that the viscous timescale is approximately a week, and maybe up to 10 days. The system parameter estimates also allowed us to determine $\dot{M}_{\text{crit}} = 1.26 \times 10^{-9} M_{\odot}/\text{yr}$ for V704 And using equation 13 in Hameury (2020, see Lasota et al. 2008),

⁸ http://www.pas.rochester.edu/~emamajek/EEM_dwarf_UBVIJHK_colors_Teff.txt

⁹ This is consistent with the mass estimated from the mass–period relation for CVs, which yields $M_2 \approx 0.33M_{\odot}$ (e.g. eq. 2.100 of Warner 1995).

which is lower than \dot{M} ; i.e. the system is expected to be in the stable regime.

Appendix D: Other VY Scl-type nova-like variables

We examined a list of VY Scl type nova-like variables in order to find similar outbursting behaviour to that observed in V704 And. In general, none of these objects show outbursts with similar nature, i.e. slower rise and faster decay. Here, we comment on a few individual objects that exhibit some kind of outburst-like event, and show the corresponding excerpts of their light curves in Fig. D.1

HV And This source exhibits one brightening event which lasts for about 30 days but has small amplitude and asymmetric shape.

V794 Aql This system shows ~ 2 mag asymmetric oscillation with an ~ 25 day period. [Honeycutt et al. \(2014\)](#) studied these stunted outbursts in more detail.

BZ Cam The measurements of BZ Cam showed a brightening event lasting for about 30 days with 0.7 mag amplitude and less symmetry.

VZ Scl This object seems to exhibit a ~ 1 mag oscillation.

LX Ser This system showed an outburst-like event in 2021 lasting for about 7 months.

CM Del The light curves of CM Del reveal a continuous outbursting behaviour with varying amplitude. We also note that some works classified this object as a DN ([La Dous 1991](#); [Lyons et al. 2001](#)).

LQ Peg A 0.4 mag outburst appeared on an ~ 25 day timescale in the photometric observations of LQ Peg.

HS 0506+7725 The light curves of HS 0506+7725 show a brightening event with ≈ 1 mag amplitude and lasting for about 40 days.

LN UMa Several brightening events occur in the light curves of LN UMa with various shapes and amplitudes. Their duration is typically 20 – 30 days.

V1082 Sgr Numerous small-amplitude brightenings are revealed by the optical light curves of V1082 Sgr.

Table D.1. List of VY Scl type nova-like variables

Object	Reference
HV And	Henden & Honeycutt (1995) Schwope & Reinsch (1992)
PX And	Warner (1995)
MV Lyr	Warner (1995)
V425 Cas	Warner (1995)
V751 Cyg	Warner (1995)
KR Aur	Warner (1995)
V794 Aql	Warner (1995)
DW UMa	Warner (1995)
LY Hya	Warner (1995)
TT Ari	Warner (1995)
BZ Cam	Warner (1995)
WX Ari	Warner (1995)
V442 Oph	Warner (1995)
VZ Scl	Warner (1995)
BH Lyn	Warner (1995)
LX Ser	Warner (1995)
CM Del	Warner (1995)
VY Scl	Warner (1995)
HS 0506+7725	Downes et al. (2001)
BH Lyn	Downes et al. (2001)
LN UMa	Downes et al. (2001)
V504 Cen	Downes et al. (2001)
V1082 Sgr	Downes et al. (2001)
RX J2337+4308	Downes et al. (2001)
TW Pic	Puebla et al. (2007)
V533 Her	Honeycutt & Kafka (2004)
FY Per	Honeycutt & Kafka (2004)
LQ Peg	Honeycutt & Kafka (2004)

TW Pic The brightness of the system is increased by ≈ 1 mag for the period of a few days.

FY Per This system shows several stunted outbursts, similarly to V794 Aql. The stunted outbursts of FY Per are discussed in [Honeycutt \(2001\)](#).

We inspected the long-term light curves of a few of the above-mentioned VY Scl-type sources using observations from AAVSO, ASAS-SN, and ZTF. We show the light curves in Figs. D.2 and D.3. For their description, see Sect. 4.3.

The Transiting Exoplanet Survey Satellite (TESS, [Ricker et al. 2015](#)) observed FY Per in 2019 December and in 2022 December with two-minute cadence, providing an ~ 26 day observing sequence for both sectors. These unprecedentedly high-cadence light curves cover one stunted outburst entirely and the decline of presumably another outburst (Fig. D.4). The 2019 measurements reveal the detailed shape of a stunted outburst with fast rise and slower decay.

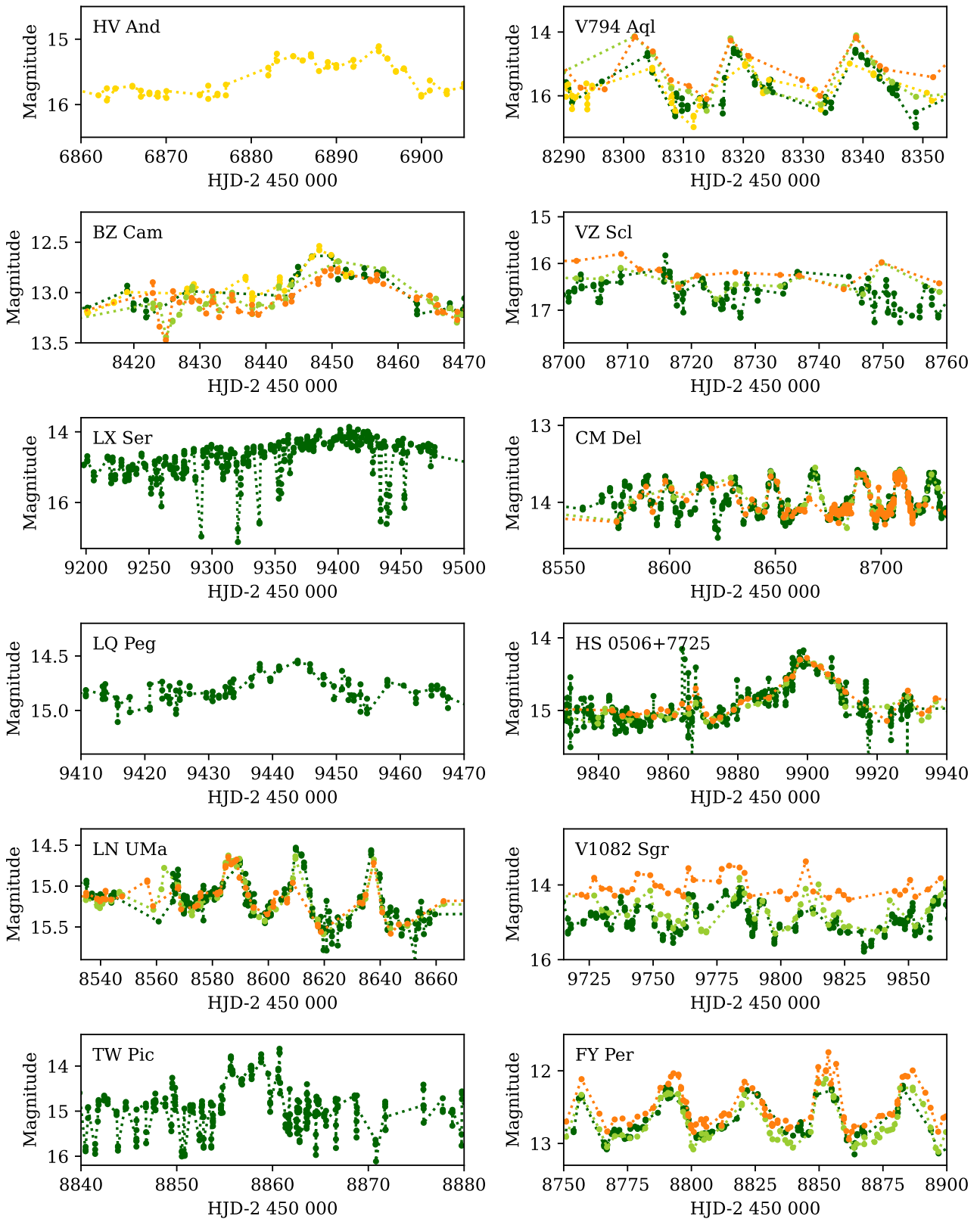


Fig. D.1. Excerpts of the optical light curves of a few VY Scl-type nova-like variables. The yellow and the dark green symbols show the ASAS-SN *V* and *g* band observations, respectively, and the orange and the light green filled circles indicate the ZTF *r* and *g* band observations. The names of the systems are displayed in the top left corner of each panel.

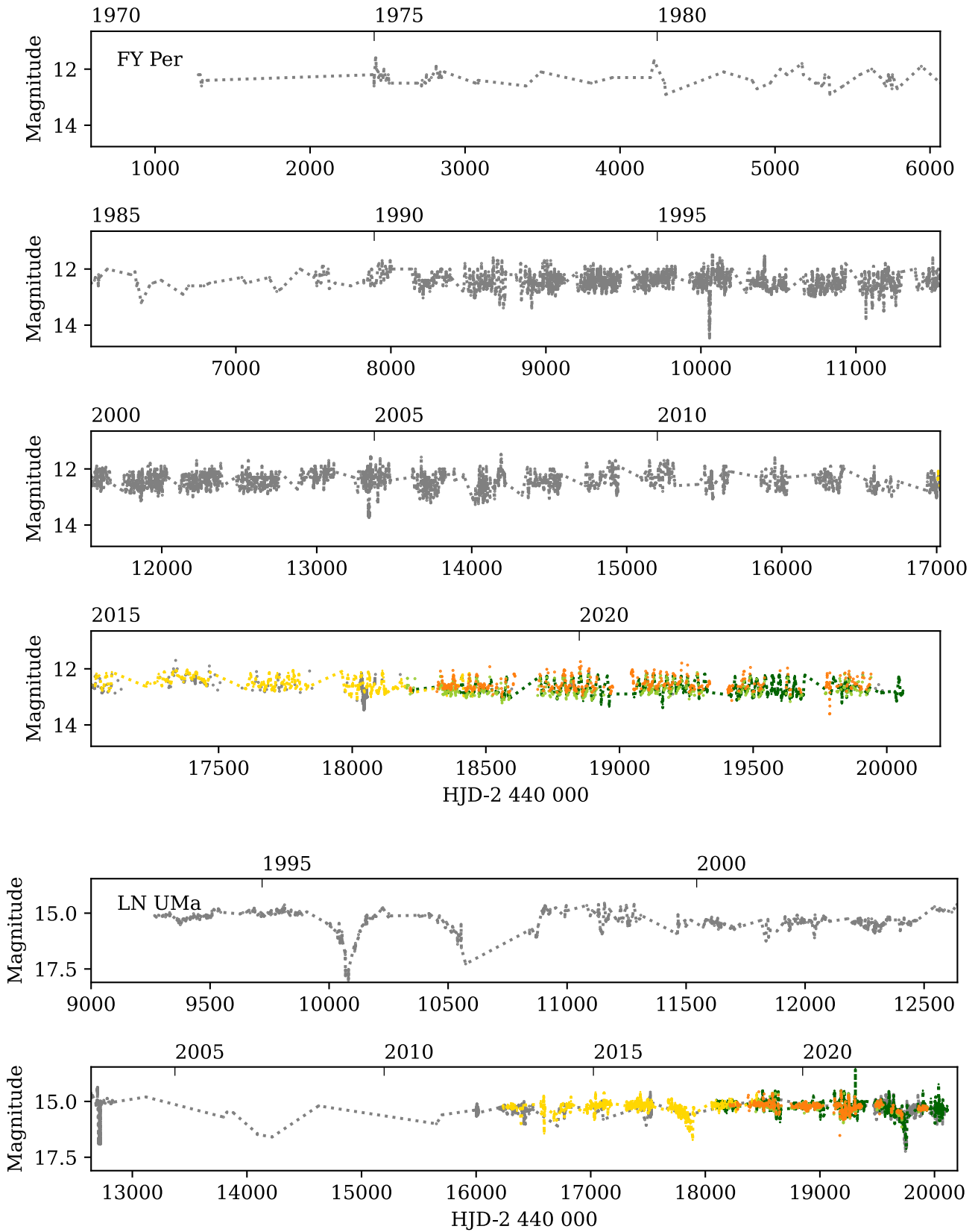


Fig. D.2. Long-term light curves of FY Per and LN UMa. The top four panels show the available AAVSO (grey), ASAS-SN *V* (yellow), ASAS-SN *g* (dark green), ZTF *r* (orange), ZTF *g* (light green) light curves for FY Per. The bottom two panels show the long-term light curves for LN UMa based on the same catalogues.

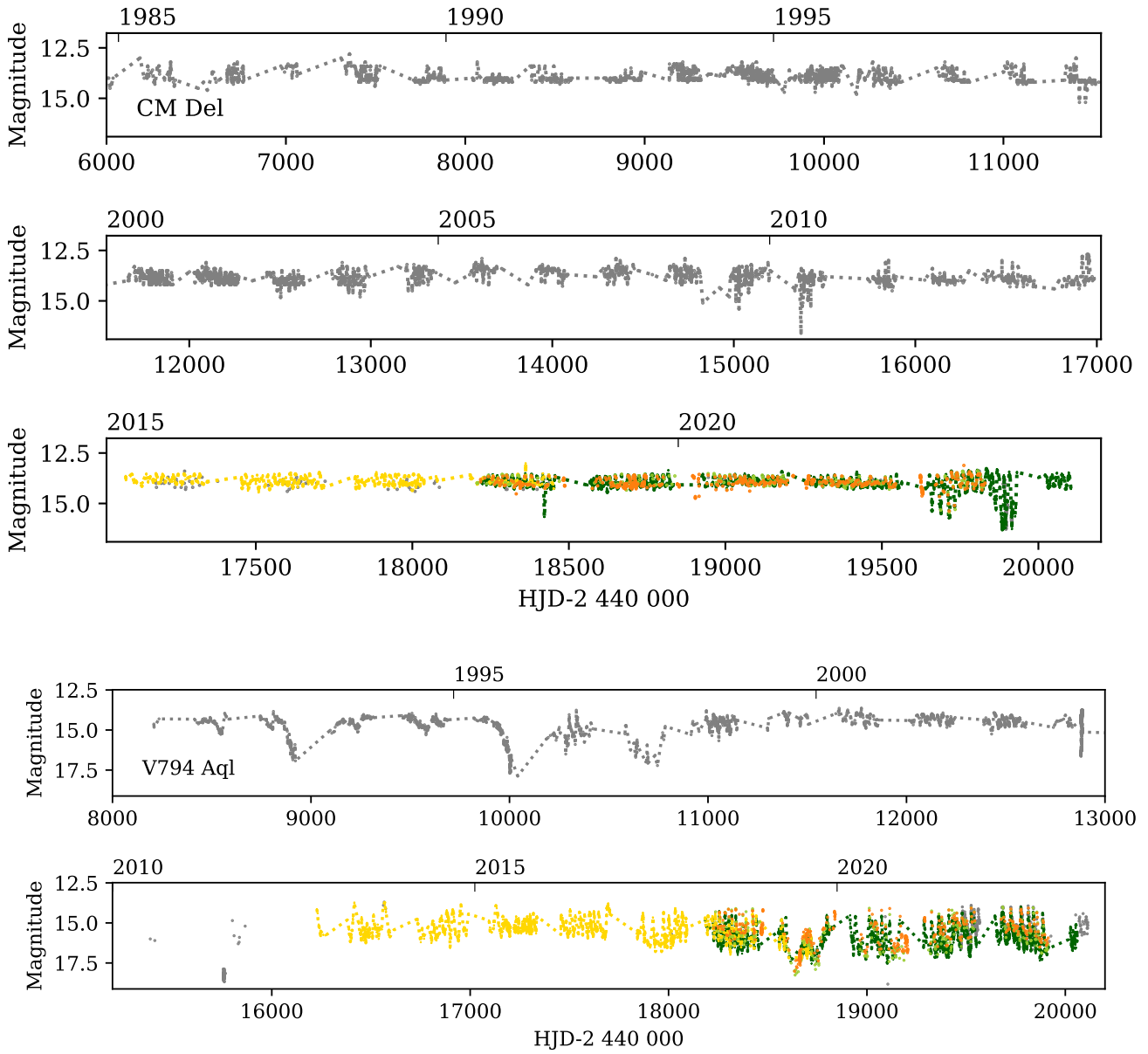


Fig. D.3. Long-term light curves of CM Del and V794 Aql. The top three panels show the available AAVSO (grey), ASAS-SN *V* (yellow), ASAS-SN *g* (dark green), ZTF *r* (orange), and ZTF *g* (light green) light curves for CM Del. The bottom two panels show the long-term light curves for V794 Aql based on the same catalogues. We note the lack of available data for the latter source between ~ 2005 and ~ 2010 .

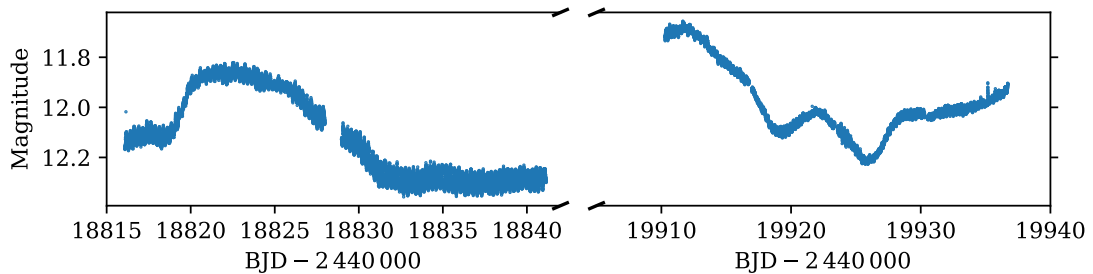


Fig. D.4. High-cadence TESS light curve of FY Per from 2019 and 2022. Both TESS Sectors provided an ~ 26 day light curve with two-minute cadence, which also reveals the $P_{orb} = 6.20$ hr (Ritter & Kolb 2003) of FY Per.

Appendix E: Swift UVOT colour–magnitude diagrams

The multifilter Swift/UVOT measurements allowed us to obtain colour–magnitude diagrams as well, which are displayed in Fig. E.1. These represent the high-state colour variations of the system.

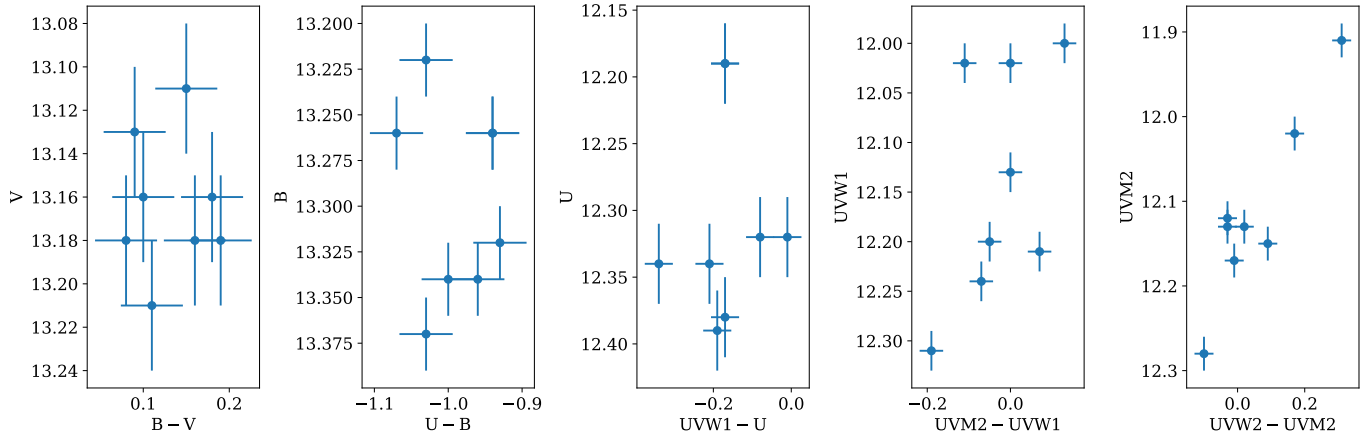


Fig. E.1. Optical and UV colour–magnitude diagrams of the Swift/UVOT measurements.